INTERNATIONAL JOURNAL FOR NUMERICAL METHODS IN FLUIDS
Int. J. Numer. Meth. Fluids 2000; **33**: 429–452

Exponential spline interpolation in characteristic based scheme for solving the advective–diffusion equation

C. Zoppou[a,*,1], S. Roberts[b] and R. J. Renka[c]

[a] *CSIRO Land and Water, Canberra, Australia*
[b] *Department of Mathematics, Australian National University, Canberra, Australia*
[c] *Department of Computer Science, University of North Texas, Denton, TX, U.S.A.*

SUMMARY

This paper demonstrates the use of shape-preserving exponential spline interpolation in a characteristic based numerical scheme for the solution of the linear advective–diffusion equation. The results from this scheme are compared with results from a number of numerical schemes in current use using test problems in one and two dimensions. These test cases are used to assess the merits of using shape-preserving interpolation in a characteristic based scheme. The evaluation of the schemes is based on accuracy, efficiency, and complexity. The use of the shape-preserving interpolation in a characteristic based scheme is accurate, captures discontinuities, does not introduce spurious oscillations, and preserves the monotonicity and positivity properties of the exact solution. However, fitting exponential spline interpolants to the nodal concentrations is computationally expensive. Exponential spline interpolants were also fitted to the integral of the concentration profile. The integral of the concentration profile is a smoother function than the concentration profile. It requires less computational effort to fit an exponential spline interpolant to the integral than the nodal concentrations. By differentiating the interpolant, the nodal concentrations are obtained. This results in a more efficient and more accurate numerical scheme. Copyright © 2000 John Wiley & Sons, Ltd.

KEY WORDS: advective–diffusion equation; finite difference scheme; shape-preserving interpolation; splines

1. INTRODUCTION

Mathematical model of the transport and fate of pollutants in aquatic systems are becoming increasingly important tools in understanding, managing, and remediating these systems. The success of these models depends on how well the physical processes in the aquatic system are described by the mathematical equations and by accuracy and efficiency with which these equations can be solved.

* Correspondence to: CSIRO Land and Water, Canberra Laboratories, Clunies Ross Street, GPO Box 1666, Canberra, ACT 2601, Australia. Tel.: +61 2 62465709; fax: +61 2 62465853.
[1] E-mail: christopher.zoppou@cbr.clw.csiro.au

Received 24 February 1998
Revised 15 August 1998

Pollutant transport processes in rivers and coastal waters are usually simulated using the advective–diffusion equation [1–4]. The advective–diffusion equation can be solved using a variety of techniques, such as finite differences [5], finite elements [6], and the method of characteristics [3]. Many of these schemes work well for smooth solutions but can produce non-physical solutions in the vicinity of rapid changes in the solution [1,3,6–8]. Lower-order numerical methods introduce artificial numerical viscosity or diffusion, which may be much greater than the physical diffusion being modeled. Higher-order polynomial-based methods are plagued by the generation of spurious oscillations or overshoots in the vicinity of steep gradients in the profile. These oscillations are non-physical and may lead to an unstable solution. Numerical methods should possess both higher-order accuracy and sharp resolution of discontinuities without excessive smearing or the introduction of spurious oscillations in the solutions.

The purpose of this paper is to present results from a numerical method similar to the method of characteristics, for the solutions of the advective–diffusion equation in one and two dimensions. The one- and two-dimensional advective–diffusion equation is solved using quasi-characteristics. This is a family of schemes for solving partial differential equations (PDEs) which only requires spatial interpolation. Shape-preserving exponential spline interpolation is used to produce solutions that capture discontinuities with no spurious oscillations and preserve the monotonicity and positivity properties of the exact solution. The authors believe that the use of shape-preserving exponential spline interpolation in characteristic based schemes has not been explored previously. This scheme will be compared with a number of numerical schemes ranging from highly diffusive first-order upwind schemes, second-order accurate schemes, monotone schemes, a third-order accurate scheme, and the fourth-order flux corrected transport (FCT) scheme. The test cases are idealized but are severe and include one- and two-dimensional pure advection problems.

In the next section, the quasi-characteristic formulation of the advective–diffusion equation is derived. In Section 3, suitable interpolation schemes that can be used in the quasi-characteristics are discussed. The use of exponential spline interpolation in the quasi-characteristic scheme is demonstrated in Section 4. In Section 5, the numerical scheme is used to solve the advection equation in two-dimensions.

2. QUASI-CHARACTERISTIC EQUATIONS

Consider the one-dimensional linear advective–diffusion equation

$$\frac{\partial c}{\partial t} + u\frac{\partial c}{\partial t} = D\frac{\partial^2 c}{\partial x^2}; \quad 0 \le x \le L, \quad t \in [0, T] \tag{1}$$

in which c is a scalar, u is the steady uniform fluid velocity, D is the constant diffusion coefficient, x is the one-dimensional co-ordinate direction, and t is time. Equation (1) can be written in the form

$$\frac{\partial c}{\partial t} = \mathscr{C}\left(x, t, \frac{\partial}{\partial x}, \frac{\partial^2}{\partial x^2}\right)c(x, t) \tag{2}$$

where $\mathscr{C}$ is a linear operator independent of the temporal derivative. For Equation (1), $\mathscr{C}$ involves two operators, $\mathscr{C} = \mathscr{L}_A + \mathscr{L}_D$, where the advection operator is $\mathscr{L}_A = -u(\partial/\partial x)$ and the diffusion operator is $\mathscr{L}_D = -D(\partial^2/\partial x^2)$.

The exact solution to Equation (2) for any interior computational node at $t + \Delta t$, given the solution at time t, can be expressed by the following Taylor series:

$$c^{n+1} = \left(1 + \Delta t \frac{\partial}{\partial t} + \frac{\Delta t^2}{2}\frac{\partial^2}{\partial t^2} + \cdots\right)c^n = \exp\left(\Delta t \frac{\partial}{\partial t}\right)c^n$$

Substituting Equation (2) into the Taylor series yields

$$\begin{aligned} c^{n+1} &= \exp(\Delta t \mathscr{C})c^n = \exp(\Delta t(\mathscr{L}_A + \mathscr{L}_D))c^n \\ &= c^n + \Delta t(\mathscr{L}_A + \mathscr{L}_D)c^n + \frac{\Delta t^2}{2}(\mathscr{L}_A^2 + (\mathscr{L}_A\mathscr{L}_D + \mathscr{L}_D\mathscr{L}_A) + \mathscr{L}_D^2)c^n + \cdots \end{aligned} \tag{3}$$

Equation (3) represents a strategy for solving Equation (1). Various schemes can be used to approximate $\exp(\Delta t(\mathscr{L}_A + \mathscr{L}_D))$ to the desired accuracy. For example, Equation (3) can be approximated by

$$c^{n+1} \approx \exp(\Delta t \mathscr{L}_A)\exp(\Delta t \mathscr{L}_D)c^n \tag{4}$$

The order of applying the two processes is unimportant. There is no restriction on the numerical schemes that can be used to solve the advection or diffusion operators. Any combination of stable methods can be used for the separate steps. A Taylor series expansion of Equation (4) reveals that it is only first-order accurate in time if $\mathscr{L}_A$ and $\mathscr{L}_D$ do not commute, otherwise it is exact. Since Equation (1) is a constant coefficient problem, then $\mathscr{L}_A$ and $\mathscr{L}_D$ commute and (4) is exact.

The first exponential $\exp[-u\Delta t(\partial/\partial x)]$ in (4) is known as a *shift operator*. For example, consider the following Taylor series

$$f(x - u\Delta t) = f(x) - u\Delta t \frac{\partial f(x)}{\partial x} + \frac{u^2\Delta t^2}{2}\frac{\partial^2 f(x)}{\partial x^2} + \cdots = \exp\left(-u\Delta t \frac{\partial}{\partial t}\right)f(x)$$

The quantity $\exp[-u\Delta t(\partial/\partial x)]$ has the effect of shifting the argument of the function from x to $x = x - u\Delta t$. Therefore, the analytical solution for the constant coefficient scalar advective–diffusion equation is simply

$$c^{n+1} = \exp\left(D\Delta t \frac{\partial^2}{\partial x^2}\right)c_\xi^n \tag{5}$$

in which $\xi = x - u\Delta t$. Expanding the diffusion operator using a Taylor series then

$$c_j^{n+1} = c_\xi^n + D\Delta t \frac{\partial^2 c_\xi^n}{\partial x^2} + \frac{D^2\Delta t^2}{2}\frac{\partial^4 c_\xi^n}{\partial x^4} + \cdots$$

Neglecting second- and higher-order terms

$$c_j^{n+1} = c_\xi^n + D\Delta t \frac{\partial^2 c_\xi^n}{\partial x^2} + O(\Delta t^2) \tag{6}$$

is the final form of the first-order quasi-characteristics formulation of the advective–diffusion equation. The advection step consists of taking the value of $c(\xi = x_j - u\Delta t, t)$ and transferring it to $(x_j, t + \Delta t)$. This is illustrated in Figure 1. Each value is then modified by the process of diffusion over the time step, Δt. Because of its similarity to a characteristic, the straight line describing the progress of the computation has been called a *quasi-characteristic* by Fenton [9]. For the constant coefficient problem, Equation (6) is also the solution to the characteristic equations for the advective–diffusion equation. Otherwise, it is a first-order approximation to the characteristics that are curved. For pure advection, this scheme is identical to semi-Lagrangian advection schemes used in numerical weather prediction [10–14].

An unusual feature of this scheme is that, unlike most finite difference schemes, it separates the processes of spatial approximation and time stepping. Equation (6) only requires spatial interpolation of the concentration c_j^n at $x = \xi$ and the evaluation of the second-derivative at the point ξ. Once the nodal values c_j^{n+1} have been estimated using Equation (6), the solution evolves by interpolating these values and solving Equation (6) for the nodal concentrations at the next time step, $n + 2$. The major practical advantages of the use of interpolation schemes are that they maintain their accuracy even for non-uniform grids. This is not generally the case for finite difference schemes. For example, the SHARP scheme is a stable third-order scheme for the solution of the advective–diffusion equation on a uniform grid, otherwise it is only first-order accurate [15]. In addition, the quasi-characteristic scheme is valid for the full range of Peclet numbers, $0 \le Pe \le \infty$, where $Pe = ul/D$, and l is a characteristic length parameter. Some numerical schemes for solving the advective–diffusion equation, such as the popular QUICK scheme [16], are unstable for the advection problem, $Pe = \infty$ [7].

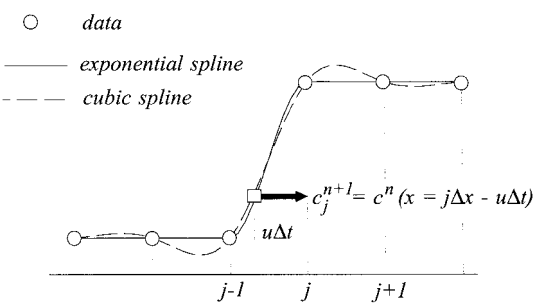

Figure 1. Interpolation in the quasi-characteristic scheme at node j, using a cubic spline and an exponential spline interpolant to data with an abrupt change, for the pure advection problem.

Any reasonable interpolation scheme may be used to solve Equation (6). The spatial interpolant must (i) be simple to implement and evaluate, (ii) be accurate, (iii) be robust, (iv) preserve the shape properties of the data, and (v) not introduce a non-physical solution.

3. INTERPOLATION SCHEMES

The use of linear interpolation to estimate the concentration at $x = \xi$ from the nodal concentrations is simply an explicit first-order upwind scheme [17]. First-order schemes are known to introduce excessive numerical diffusion. Higher-order interpolation schemes are preferable. Simple polynomials are not suitable for this problem because of the large number of function values a polynomial of large degree may require. Interpolation error also increases with increasing polynomial degree. This can be avoided by using low-order polynomials over small sub-intervals and not over the whole computational domain. This leads to *piecewise polynomial interpolation*.

There are a number of piecewise interpolation polynomials, such as Lagrange, Hermite, and splines. Lagrange interpolants satisfy the pure interpolatory condition [18]. However, the interpolant is only $C^0[x_j, x_{j+1}]$ and linear Lagrange interpolation is very diffusive [19,20]. A higher-order polynomial is required to obtain a smoother interpolant over the sub-interval $[x_j, x_{j+1}]$. Hermite interpolants not only fit a polynomial to the function values but also interpolate a given number of consecutive derivatives at each computational point. The simplest Hermite interpolant is the *cubic Hermite polynomial*, which demands that the function values and the first derivative are satisfied in each sub-interval. This results in a $C^1[x_j, x_n]$ interpolant. The major advantages of cubic Hermite interpolation are that the interpolant is simple to implement and can be constructed using only information within each sub-interval.

One of the first attempts to use cubic Hermite interpolants in a characteristic scheme for the solution of the advective–diffusion equation is due to Holly and Preissmann [3]. Since the nodal concentrations and their derivatives are required to fit a cubic Hermite interpolant, both the concentration and derivatives are treated as dependent variables. Therefore, in this scheme, the advection of the derivatives, which is an auxiliary problem, must be solved. This is sufficient to solve the advection equation. Second and third derivatives of the interpolation polynomial are required for the diffusion operator. These are estimated by differentiating the interpolant. Since the interpolation polynomial used was the cubic Hermite, which is only C^1, it is not surprising that the cubic Hermite interpolant was found to provide inconsistent estimates of the higher derivatives at the nodes, resulting in poor model performance. Yang *et al.* [21] attempted to overcome this problem by using quintic Hermite interpolation. In the pure advection case, the concentration, first and second derivatives are considered as dependent variables. For the advective–diffusion equation, continuity of the second derivative is ensured but continuity of the third derivative was assumed.

To avoid the problem of estimating the second and third derivatives required by the Holly and Preissmann scheme for the solution of the advective–diffusion equation, the operator splitting scheme has been proposed [22–25]. The advection operator is solved using the Holly and Preissmann scheme and the diffusion operator is solved using finite differences.

Instead of fitting a C^1 interpolant, which uses local information only, it is possible to fit a C^2 global interpolant, such as a cubic spline. Splines satisfy the interpolatory conditions and continuity of derivatives at the nodes. For the C^2 cubic spline, continuity of the first and second derivative is satisfied at the nodes. These have been used by Schohl and Holly [26] to solve the advection equation. Like cubic Hermite interpolants, extraneous inflection points usually occur in the interpolant in the vicinity of rapid changes in the data; see, for example, the cubic spline interpolation of the data shown in Figure 1. In all the above studies, negative concentrations and oscillations in the solutions in the solution, which are artifacts of the numerical scheme, could not be avoided.

It is important that properties of the data, such as *positivity*, *monotonicity*, or *convexity*, are preserved and that the interpolant does not introduce extraneous extrema often seen in many standard interpolation schemes [27]. These are very desirable properties, which a numerical scheme should also possess. Shape preserving interpolants have been developed, which attempt to preserve the properties of the data. These include *monotone cubic Hermite interpolants* [27–29], *taut splines* [30], and *exponential splines* [27,31–35].

In many practical applications, the derivatives at the computational nodes that are required by cubic Hermite interpolants are not known and hence must be determined from the data. How these derivatives are calculated will influence the final shape of the interpolant. Using simple finite differences for estimating the nodal derivatives in a cubic Hermite interpolant results in a scheme that produces overshoots and undershoots in the vicinity of steep gradients. Strategies have been developed recently for estimating the nodal derivatives in an attempt to avoid the production of these spurious oscillations. Methods for estimating the nodal derivatives at the abscissa required by the cubic Hermite interpolant can be found in Fritsch and Carlson [28], Fritsch and Butland [29], Akima [36], Hyman [37,38], and Huynh [39]. Hyman's method is designed for accuracy, while the methods of Akima, Fritsch and Carlson, Fritsch and Butland, and Huynh are designed to preserve the shape properties of the data. All these methods employ local information to estimate the nodal derivatives. Therefore, it is difficult for these algorithms to distinguish between local extrema and extrema in the data. Clipping of extrema in the data by these schemes produces results that resemble a highly diffusive numerical scheme (see, for example, Zoppou [40]). Fritsch and Carlson's monotone cubic Hermite interpolation, although very efficient, introduces excessive phase errors because the monotone preserving strategy is not symmetric.

Using only local information will produce a C^1 monotone preserving cubic Hermite interpolant, which could be used in a characteristic based scheme for the solution of the advection equation. However, the C^1 cubic Hermite interpolant will not provide continuous second derivatives required by Equation (6). A C^2 interpolant is required in this case.

Through an appropriate selection of additional nodes or knots between the data abscissa, de Boor [30] produces a taut spline, which is a cubic spline that preserves convexity of the data. Unfortunately, in the taut spline there is no control on the position of these additional knots. Numerical experiments have shown that there is an abrupt change in the second derivative of the interpolant near these additional nodes [40]. Therefore, its use in a characteristic based scheme for the solution of the advective–diffusion equation is not recommended.

3.1. Exponential splines

A third method of constructing a shape preserving interpolant is provided by exponential splines, also known as tension splines. Exponential splines and interpolants can be made arbitrarily close to the piecewise linear interpolant, while retaining two continuous derivatives, using tension factors. A function E: $[x_1, x_n] \to \mathbb{R}$ is called an exponential interpolant with knots x_j if (i) $E(x) \in C^2[x_1, x_n]$; (ii) $E(x_j) = y_j$ for $j = 1, \ldots, n$; and (iii) it minimizes the integral

$$\sum_{j=1}^{n-1} \int_{x_j}^{x_{j+1}} [E''(x)]^2 + \lambda_j^2 [E'(x)]^2 \, \mathrm{d}x \tag{7}$$

for $x = [x_j, x_{j+1}]$, $j = 1, \ldots, n-1$. The parameter λ_j is the non-negative tension factor, which governs the steepness of the resulting interpolant. The function that minimizes Equation (7) must satisfy

$$E''''(x) - \lambda_j^2 E''(x) = 0 \tag{8}$$

on $x \in [x_j, x_{j+1}]$, $j = 1, \ldots, n-1$. With the natural boundary conditions $E''(x_1) = E''(x_n) = 0$, this corresponds to an interpolation function with a linear variation of the quantity $E''(x) - \lambda_j^2 E(x)$, $x \in [x_j, x_{j+1}]$. The property Equation (8) is analogous to minimizing the energy function of a bending rod subject to the action of tensile forces. The parameters λ_j are proportional to the tensile force [32].

A function $E(x)$, where $E''(x) - \lambda_j^2 E(x)$ is linear in each sub-interval $[x_j, x_{j+1}]$ is obtained by solving

$$E''(x) - \lambda_j^2 E(x) = [E''(x_j) - \lambda_j^2 y_j]\delta + [E''(x_{j+1}) - \lambda_j^2 y_{j+1}](1 - \delta) \tag{9}$$

where $\delta = (x - x_j)/\Delta x$, $\mu_j = \lambda_j \Delta x$. Using condition (ii) then the solution to Equation (9) is a unique linear combination of basis functions $\{1, x, \mathrm{e}^{\lambda_j x}, \mathrm{e}^{-\lambda_j x}\}$. A local representation of $E(x)$ is given by Rentrop [32] as

$$E(x) = a_j + b_j(x - x_j) + c_j \, \mathrm{e}^{\lambda_j (x - x_j)} + d_j \, \mathrm{e}^{-\lambda_j (x - x_j)} \tag{10}$$

with constants a_j, b_j, c_j, and d_j.

The numerical properties of Equation (10) do not behave well for the limiting cases $\lambda_j \to 0$ and $\lambda_j \to \infty$. It is more convenient to use hyperbolic functions, which have stable numerical properties. The exponential spline becomes [32]

$$E(x) = y_{j+1}\delta + y_j(1 - \delta) + \frac{y''_{j+1}}{\lambda_j^2}\left[\frac{\sinh(\mu_j \delta)}{\sinh(\mu_j)} - \delta\right] + \frac{y''_j}{\lambda_j^2}\left[\frac{\sinh(\mu_j(1 - \delta))}{\sinh(\mu_j)}(1 - \delta)\right] \tag{11}$$

where $\Delta x = x_{j+1} - x_j$. Satisfying continuity of the first derivative, obtained by differentiating Equation (11) for the $j = 2, \ldots, n-1$ abscissa produces a definite tridiagonal system of equations. These equations are solved for the unknown second derivative y''_j with the use of appropriate boundary conditions.

If $\lambda_j = 0$, the exponential spline reduces to a linear combination of the basis functions $\{1, x, x^2, x^3\}$ characteristic of C^2 cubic splines, which satisfy the differential equation $E''''(x) = 0$, $\forall x \in [x_1, x_n]$. A piecewise linear C^0 interpolant is produced when $\lambda_j = \infty$, which preserves the positivity, monotonicity, and convexity of the data. Therefore, it is reasonable to choose the tension factors λ_j to be small as possible, but sufficiently large to remove unwanted extraneous extrema in the polynomial. The lack of a general and efficient method for selecting the tension factors required to produce a shape preserving interpolant, which also preserves the positivity of the data, has greatly diminished the practical application of exponential splines in evolution problems. Cline [31] used uniform tension factors that must be specified. Rentrop [32] describes a simple method for estimating the tension factors that eliminates oscillations in the interpolant. Unfortunately, the method is not very robust. Rentrop and Wever [33] use an optimization strategy to estimate the tension factors that preserve the convexity of the data only. Wever [35] estimates the tension using a computationally expensive non-linear constrained optimization strategy, which will preserve the positivity of the data. Renka [27] developed an iterative method for selecting the tension factors that will produce either a C^1 or C^2 exponential interpolant that preserve certain properties of the data.

Renka relaxed the continuity requirement of the exponential interpolant. A function $E(x) \in C^1[x_1, x_n]$, where $E''(x) - \lambda_j^2 E(x)$ is linear in each sub-interval $x \in [x, x_{j+1}]$ was sought. Using the basis functions $\{1, x, \text{coshm}(\lambda_j, \delta), \text{sinhm}(\lambda_j, \delta)\}$, which have stable numerical properties and $\lambda_j > 0$, the exponential interpolant is given by [22]

$$P(x) = y_{j+1} - y'_{j+1}\Delta x_j(1-\delta) + \frac{\Delta x_j}{\lambda_j \alpha_1}(\alpha_1 \,\text{coshm}(\lambda_j(1-\delta)) - \alpha_2 \,\text{sinhm}(\lambda_j(1-\delta))) \tag{12}$$

where $\text{sinhm}(z) = \sinh(z) - z$, $\text{coshm}(z) = \cosh(z) - 1$, $\alpha_1 = \lambda_j \,\text{coshm}(\lambda_j)(y'_{j+1} - \Delta_j) - \text{sinhm}(\lambda_j)(y'_{j+1} - y'_j)$, $\alpha_2 = \lambda_j \sinh(\lambda_j)(y'_{j+1} - \Delta_j) - \text{coshm}(\lambda_j)(y'_{j+1} - y'_j)$, $\alpha_3 = \lambda_j \sinh(\lambda_j) - 2(\text{coshm}(\lambda_j))$ and $\Delta_j = (y_{j+1} - y_j)/\Delta x_j$. Renka showed that Equation (12) is a cubic interpolant when $\lambda_j = 0$. The fourth-order monotonicity constrained parabolic method of Hyman [38] is used to obtain local derivative estimates. Minimum tension factors are determined iteratively using a nonlinear equation solver so that the interpolant satisfies locally defined properties, such as monotonicity, convexity, or to satisfy more general bounds on function values and derivatives in each subinterval. This will produce a monotone preserving C^1 exponential interpolant given by Equation (12), which is satisfactory for the solution of the advection equation in characteristic based schemes. For the solutions of the advective–diffusion equation, accurate estimates of the second derivative are required. A global C^2 exponential interpolant is obtained by satisfying continuity of the second derivative at the knots. For $j = 2, \ldots, n-2$, Equation (12) will result in $n-2$ linear equations for the n unknown nodal derivatives y'_j of the form

$$\begin{aligned}&[g_2(\lambda_{j-1}) - g_1(\lambda_{j-1})]y'_{j-1} + [g_1(\lambda_{j-1}) - g_1(\lambda_j)]y'_j + [g_2(\lambda_j) - g_1(\lambda_j)]y'_{j+1} \\ &= g_2(\lambda_{j-1})\Delta_{j-1} + g_2(\lambda_j)]\Delta_j\end{aligned} \tag{13}$$

where

$$g_2(\lambda) = \begin{cases} (\lambda/(\alpha_3 \Delta x))[\lambda \ \mathrm{coshm}(\lambda) - \mathrm{sinhm}(\lambda)] & \text{if } \lambda > 0 \\ 4/\Delta x & \text{if } \lambda = 0 \end{cases}$$

and

$$g_2(\lambda) = \begin{cases} (\lambda^2 \ \mathrm{coshm}(\lambda))/(\alpha_3 \Delta x) & \text{if } \lambda > 0 \\ 6/\Delta x & \text{if } \lambda = 0 \end{cases}$$

Two additional equations are required, which are provided by the boundary conditions. For a C^2 exponential spline interpolant, iteration alternates between (i) computing minimum tension factors for a given set of nodal first derivatives so that certain properties, such as monotonicity, convexity, and positivity of the data are preserved, and (ii) satisfying continuity of the second derivative at the nodes by solving a system of linear equations, Equation (13) for the nodal first derivatives using a given set of tension factors. Beginning with zero tension factors, the iteration ceases when there is no increase in the estimated tension factors in each sub-interval. When the nodal derivatives and tension factors are known, the C^2 exponential interpolant is given by Equation (12), which is a compromise between a shape-preserving interpolant and a smooth spline. This approach utilized the wealth of information that exists on obtaining nodal derivatives, which preserve the characteristics of the data. A computer implementation of the shape preserving exponential spline interpolation is available in Renka [41], which was used to fit a C^2 exponential spline interpolant through the data given in Figure 1. Unlike the cubic splines there are no extraneous extrema introduced by the exponential spline interpolant.

The exponential spline interpolant requires as boundary conditions, the nodal values and either an estimate of the first or second derivative. One-sided difference schemes [42] can be used to provide estimates of the boundary derivatives. For the first derivative to retain third-order accuracy of the scheme in the interior, the first derivative must be approximated to at least second-order accuracy, and the second derivative to at least first-order accuracy. Therefore, for advection, the scheme will retain its third-order accuracy. Since the second derivative is needed for the advective–diffusion equation, the scheme is only formally first-order accurate, which is consistent with the time stepping.

We examine the use of exponential spline interpolation in a quasi-characteristic scheme for the solution of the one-dimensional advective-diffusion equation.

4. ONE-DIMENSIONAL PROBLEM

The behavior of the quasi-characteristic scheme with exponential interpolation will be compared with several well-known numerical schemes for modeling the one-dimensional advective–diffusion equation. The first example is the advection $Pe = \infty$ of a simple test profile given by

$$c(x, t=0) = \begin{cases} 100 & \text{for } 0 \le x \le 5\Delta x \\ 100 \sin^2(\pi x/20\Delta x) & \text{for } 25\Delta x \le x \le 45\Delta x \\ 0 & \text{for } 45\Delta x < x \le L = 100 \text{ m} \end{cases}$$

which consists of step and a sine-squared of width $20\Delta x$. The fluid velocity $u = 0.5$ m s^{-1} and $\Delta x = 1$ m, $\Delta t = 1$ s; therefore, the numerical Courant number is $Cr = u\Delta t/\Delta x = 0.5$. The simulated and analytical profile are compared at time $T = 100$ s. The analytical solution to this problem is simply the advection of the profile at the speed u, without deformation.

Results were obtained for this problem using (i) first-order upwind scheme [43] as shown in Figure 2(a); (ii) second-order Lax–Wendroff scheme [44] shown in Figure 2(b); (iii) the Warming–Beam scheme [45] illustrated if Figure 2(c); (iv) the third-order Holly and Preissmann scheme [3], which is shown in Figure 2(d); (v) the fourth-order FCT [46] scheme of Morrow and Noye [47] with Zalesak's [48] flux limiter as shown in Figure 2(e); and (vi) Leonard's third-order ULTIMATE–QUICKEST scheme [49] shown in Figure 2(f). The results obtained using quasi-characteristics with cubic splines, quintic splines [50], and exponential interpolation are shown in Figure 3(a)–(c) respectively.

The highly diffusive first-order upwind scheme, while producing monotone preserving results, has smeared the step function and significantly diffused the smoother sine-squared profile. The second-order schemes, Lax–Wendroff, and Warming–Beam schemes, introduce a dispersion that manifests itself as oscillations in the solution near abrupt changes in the concentration profile. Form Figure 1(b) and (c) it is apparent that the dispersion errors produce strong leading waves with the second-order Warming–Beam scheme and strong trailing waves with the Lax–Wendroff scheme. The location of these waves is dependent on the sign of the dispersion coefficient in the modified equivalent partial differential equation [51], which for these schemes is a dispersion equation. The behavior of second-order schemes can be predicted from the properties of the analytical solution to the dispersion equation, which can be expressed in terms of Airy's function [40]. The dispersion coefficient is negative for the Warming–Beam scheme, resulting in leading waves, whereas it is positive for the Lax–Wendroff scheme, which produces trailing waves. Dispersion terms may still cause overshoots and undershoots in the vicinity of steep gradients in higher-order schemes. This is the case for the Holly and Preissmann scheme, which is a third-order scheme (see Figure 2(d)). The analytical solution of the modified equivalent PDE for third-order schemes shows that oscillations should occur both leading and trailing the discontinuity and that they are symmetrical about the discontinuity. This has occurred in the results shown in Figure 2(d). In this scheme negative concentrations were also obtained for the smoother sine-squared profile.

The use of flux or slope limiters in a numerical scheme has produced results that remain positive and provide a sharp resolution of the discontinuity and the smoother profile. In Figure 2(e), the flux limiter of Zalesak has clipped the smoother sine-squared profile and its resolution of this profile is poorer than the Holly and Preissmann scheme. The ULTIMATE–QUICKEST scheme, shown in Figure 2(f), produces excellent resolution of the smoother sine-squared profile, but its resolution of the shock is not as sharp as that produced by the FCT scheme. However, neither of these schemes resolve the discontinuity to the same accuracy as the Holly and Preissmann scheme. Quasi-characteristic with cubic Hermite interpolation, which is a third-order scheme, produced results that are very similar to the Holly and Preissmann scheme.

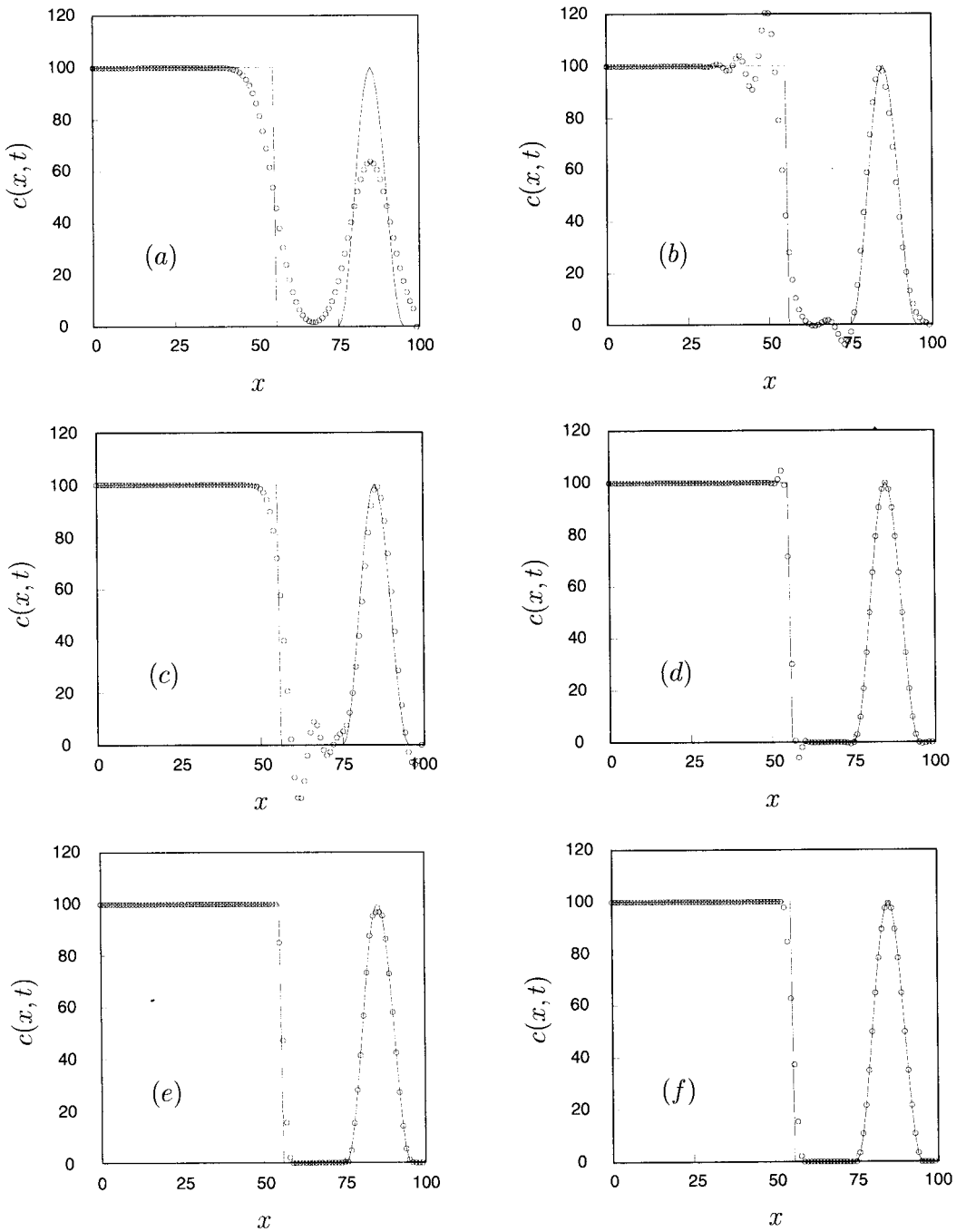

Figure 2. Solution of the advection equation where $Cr = 0.5$ using (a) first-order upwinding, (b) Lax–Wendroff, (c) Warming–Beam, (d) Holly and Preissmann, (e) FCT, and (f) ULTIMATE–QUICKEST schemes.

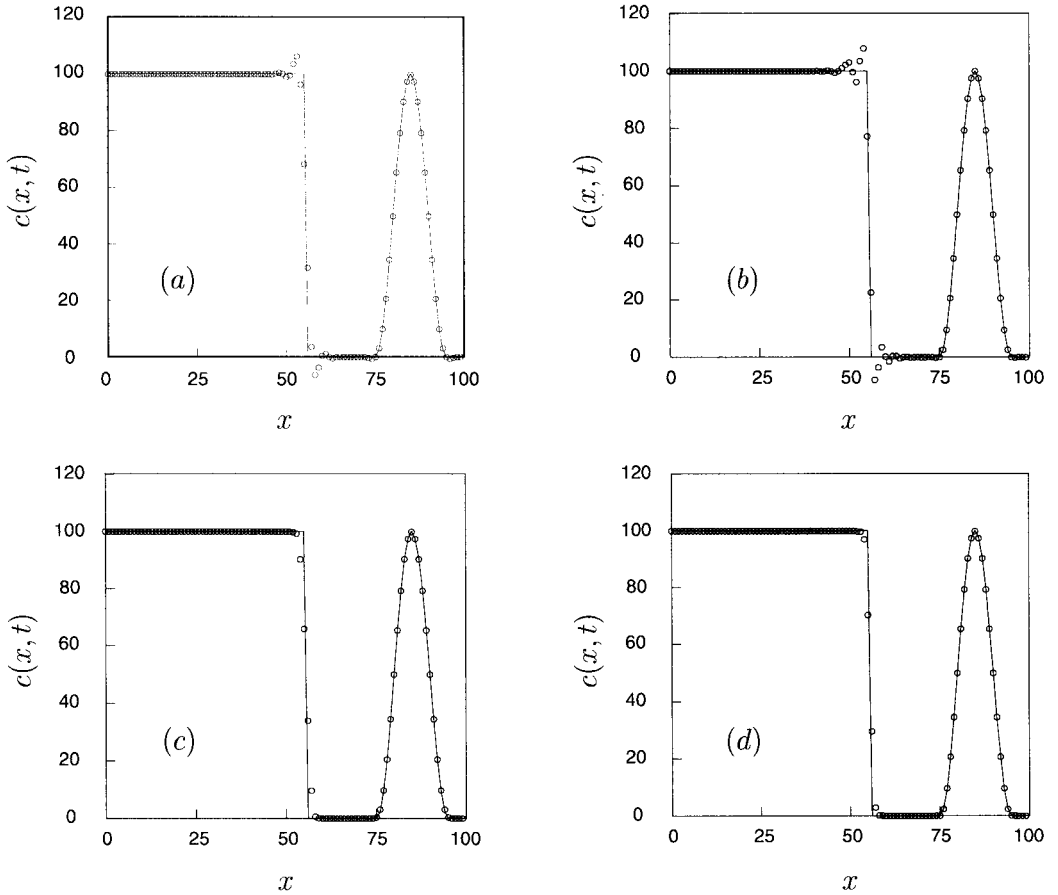

Figure 3. Solution of the advection equation where $Cr = 0.5$ using quasi-characteristics with (a) cubic Hermite, (b) quintic splines, (c) exponential spline interpolation, and (d) exponential spline interpolation fitted to the integral of the concentration profile.

There is excellent resolution of the discontinuity, but the scheme introduces spurious oscillations near abrupt changes in the profile (see Figure 3(a)). The use of quintic splines in the quasi-characteristic scheme, shown in Figure 3(b), provides the best resolution of the discontinuity and smoother profile. This fifth-order scheme however, is still plagued by spurious oscillations in the solution. These oscillations have higher amplitude and pollute a greater region of the solution than the oscillations produced by the Holly and Preissmann scheme and the quasi-characteristic scheme with cubic Hermite interpolation. Oscillations are avoided and the solutions remains positive when exponential spline interpolation is used in the quasi-characteristics scheme. The results shown in Figure 3(c) for this scheme have produced reasonable resolution of the discontinuity. Resolution is better than the ULTIMATE–QUICKEST scheme, but not as accurate as either the FCT or the Holly and Preissmann schemes.

Instead of fitting an exponential interpolant to the concentration profile, it was fitted to the integral of the concentration profile I_j^n at the time $n\Delta t$, which is defined as

$$I_j^n = \int_0^{x_j} c(x, n\Delta t)\, \mathrm{d}x$$

It is computationally less expensive to fit an exponential spline interpolant to the integral of the concentration profile, which is smoother than the concentration profile. The integral of the concentration I_j^n is treated as the dependent scalar variable in Equation (6). This is similar to the approach used by Holly and Priessmann [3], where the nodal derivatives required by the cubic Hermite interpolant were also treated as dependent variables and it is similar to the NIRVANA scheme [52], where the cumulated sum of the cell average values is fundamental to this scheme. In the quasi-characteristic scheme, the cumulative nodal values are used instead and like the NIRVANA scheme, the use of the integral of the concentration guarantees conservation. This is not the case when the concentration is used in the quasi-characteristic scheme.

The nodal concentrations c_j^n are obtained by differentiating the interpolant that has been fitted through the integral of the concentration profile I_j^n. Therefore, for the constant coefficient advection problem, the scheme has second-order accuracy and for the advective–diffusion equation it has first-order accuracy. The results produced by the quasi-characteristic scheme with exponential interpoltion of the integral of the concentration profile is shown in Figure 3(d). No new local extrema are created. The results remain positive and the discontinuity is resolved to approximately the same accuracy of the quintic spline and the Holly and Preissmann scheme. Overall it is a more robust numerical scheme in comparison to all the others used in this example.

4.1. Quantifying the performance of various schemes

To quantify the performance of the various methods for solving the advective–diffusion equation, the minimum, the maximum simulated concentration, and the normalized L_1-norm between exact and simulated profile have been calculated for another test profile. The normalized L_1-norm is defined as

$$L_1 = \frac{\sum_{j=1}^{k} |c_j - C(x_j)|}{\sum_{j=1}^{k} |C(x_j)|} \tag{14}$$

in which the first moment of the approximate solution c_j, evaluated using the solution obtained at time t at all the k computational nodes in the domain, $j = 1, \ldots, k$, is normalized by the corresponding exact solution $C(x_j)$.

The concentration profile in the second example is given by

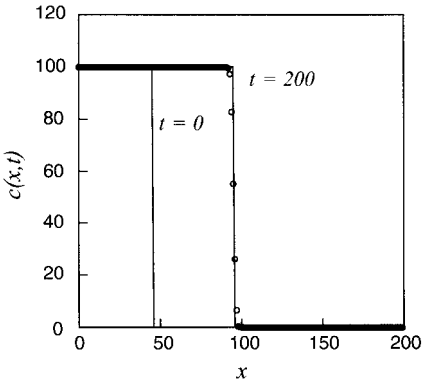

Figure 4. Initial exact and quasi-characteristic scheme with exponential spline interpolation solution to the advection problem, where $Cr = 0.25$.

$$c(x, t = 0) = \begin{cases} 100 & \text{for } 0 \le x \le 45\Delta x \\ 0 & \text{for } 45\Delta x < x \le L = 200 \text{ m} \end{cases} \tag{15}$$

In each numerical scheme $\Delta t = 1$ s, $\Delta x = 1$ m, and $u = 0.25$ m s^{-1}; therefore, $Cr = 0.25$. The solution is sought at time $T = 200$ s, after which the concentration profile has traveled to the location $x = 95$ m without deformation. The initial profile the exact solution and the results obtained from the quasi-characteristic scheme using exponential spline interoplation are illustrated in Figure 4.

The minimum, $c_{\min}$, maximum $c_{\max}$, and L_1-norm, defined by Equation (14), were evaluated for all the numerical schemes used in the first example. These are given in Table I along with the relative computational time required by each scheme.

Table I. Minimum, maximum, L_1-norm, and relative execution time for the solution of the one-dimensional advection equation of a step profile for various schemes.

Numerical scheme	Minimum, $c_{\min}$	Maximum, $c_{\max}$	L_1	Relative CPU time
First-order upwinding	0.000	100.000	0.508043×10^{-1}	1.000
Lax–Wendroff	0.000	124.678	0.397442×10^{-1}	1.165
Warming–Beam	−19.534	100.000	0.354703×10^{-1}	1.165
Holly and Preissmann	−6.249	103.500	0.969364×10^{-2}	1.671
FCT	0.000	100.000	0.804587×10^{-2}	4.778
ULTIMATE–QUICKEST	0.000	100.000	0.123384×10^{-1}	1.603
Characteristics with				
Cubic Hermite	−3.573	109.137	0.113015×10^{-1}	4.603
Quintic splines	−4.941	109.831	0.983326×10^{-2}	21.342
Exponential spline	0.000	100.000	0.102501×10^{-1}	153.641
Integral	0.000	100.000	0.705714×10^{-2}	59.035

Only numerical schemes that use some form of flux or slope limiter avoid the generation of spurious extrema. All the other schemes introduce oscillations in the solution resulting in negative concentrations and spurious extrema is the solution. This is not the case for the first-order scheme, which is the least costly scheme, but is also the least accurate because it is a highly diffusive scheme. The cost associated with the FCT scheme is not unexpected. In this scheme, the problem is solved using two numerical schemes. Compared with cubic Hermite interpolants, the use of higher-order quintic spline interpolation in the quasi-characteristic scheme has not significantly improved the accuracy of the scheme. There seems to be no advantage in using higher-order interpolation, such as quintic splines, in a characteristic based scheme, unless some form of shape-preserving strategy can be employed. Satisfactory results can be obtained using cubic intepolants. The use of exponential spline interoplation has preserved the properties of the data at a cost. It is computationally the most expensive scheme. However, it is not plagued with the obvious problems associated with the Holly and Preissmann and quasi-characteristic scheme using cubic Hermite interpolation or quintic splines. A significant improvement in both accuracy and computational effort was obtained when an exponential interpolant was fitted to the integral of the concentration profile in the quasi-characteristic scheme. It is the most accurate scheme, providing results exceeding the accuracy of both the fourth-order FCT scheme and the fifth-order quintic spline scheme. More importantly, it preserves the properties of the exact solution.

The computational effort required to solve the quasi-characteristic based scheme is at least an order of magnitude greater than many of the other schemes. However, with the exponential growth in computer speed, the time required to solve a numerical scheme is becoming less relevant in the choice of a numerical scheme. The accuracy of a numerical scheme cannot be improved by computer resources alone. Therefore, the criterion used to assess the accuracy of the new scheme is its accuracy compared with a number of other well-known schemes and not only on the computational time required to solve the numerical scheme.

The third example is solved using first-order upwind, second-order Lax–Wendroff, the Holly and Preissman scheme, the FCT scheme, and quasi-characteristics with cubic Hermite quintic splines, and the exponential spline interpolant fitted to both the nodal concentrations and to the integral of the concentration profile. The concentration profile is given by

$$c(x, t=0) = \begin{cases} 100 & \text{for } 0 \le x \le x_0 \\ 0 & \text{for } x_0 < x \le L = 200 \text{ m} \end{cases}$$

In each numerical scheme $\Delta t = 1$ s, $\Delta x = 1$ m, and $u = 0.5$ m s^{-1}; therefore, $Cr = 0.5$, $x_0 = 5$, $D = 0.1$ and 0.01. This satisfies the stability constraints for all schemes and $Pe = 5$ and 50, where $Pe = u\Delta x/D$ and Δx is the grid spacing. The solution is sought at time $T = 100$ s after which the concentrations profile is given by [4]

$$C(x, t) = \frac{c_0}{2}\operatorname{erfc}\left[\frac{x - ut - x_0}{2\sqrt{Dt}}\right] + \frac{c_0}{2}\exp\left[\frac{u(x - x_0)}{D}\right]\frac{c_0}{2}\operatorname{erfc}\left[\frac{x + ut - x_0}{2\sqrt{Dt}}\right]$$

When $Pe \neq \infty$, diffusion may attenuate the oscillations that are introduced in a numerical scheme. Therefore, only the L_1-norm is provided as a measure of the performance of a numerical scheme when $Pe \neq \infty$. These have been provided in Table II for $Pe = 5$, and Table III for $Pe = 50$.

Although most of the schemes produced results that were indistinguishable from the analytical solution for $Pe = 5$, this was not the situation for the solution of the advective–diffusion equation for $Pe = 50$. Some of these schemes introduce non-physical results. This is evident from the L_1-norm given in Tables II and III. When $Pe = 5$, the concentration profile is relatively smooth. All the schemes are free from oscillations in the solution and provide consistent values for the L_1-norm. This is also the case for the higher-order schemes when $Pe = 50$. The only exceptions are the first-order upwinding and the quasi-characteristic scheme using exponential spline interpolants fitted to the integral of the concentration profile. The first-order scheme introduces numerical diffusion, which dominates the large physical diffusion

Table II. The L_1-norm and relative execution time for the solution of the one-dimensional advective–diffusion equation of a step profile using various schemes with $Pe = 5$.

Numerical scheme	L_1	Relative CPU time
First-order upwinding	0.181114×10^{-1}	1.000
Lax–Wendroff	0.297914×10^{-2}	1.054
Holly and Preissmann	0.297016×10^{-2}	1.374
FCT	0.297915×10^{-2}	2.651
Quasi-characteristics with		
Cubic Hermite	0.297915×10^{-2}	2.566
Quintic splines	0.297919×10^{-2}	9.048
Exponential spline	0.297915×10^{-2}	42.089
Integral	0.197630×10^{-2}	16.594

Table III. The L_1-norm and relative execution time for the solution of the one-dimensional advective–diffusion equation of a step profile using various schemes with $Pe = 50$.

Numerical scheme	L_1	Relative CPU time
First-order upwinding	0.302424×10^{-1}	1.000
Lax–Wendroff	0.145948×10^{-1}	1.054
Holly and Preissmann	0.519665×10^{-2}	1.377
FCT	0.500343×10^{-2}	2.590
Quasi-characteristics with		
Cubic Hermite	0.528221×10^{-2}	2.536
Quintic splines	0.498490×10^{-2}	8.954
Exponential spline	0.498756×10^{-2}	48.275
Integral	0.115914×10^{-2}	18.674

in this problem. Oscillations are produced by the dissipative Lax–Wendroff scheme when $Pe = 50$. The use of the exponential spline interpolation in the quasi-characteristic scheme produces results that are competitive to other schemes, which employ some form of flux or slope limiter. Unfortunately, it is the most expensive scheme. Fitting an exponential interpolant to the integral of the concentration profile produces a numerical scheme that is consistently more accurate for the full range of Peclet numbers than all the other schemes used in this study. However, this scheme is also computationally expensive.

From the above examples, the use of quasi-characteristics with exponential interpolants fitted to the integral of the concentration profile, consistently provides the most accurate results. Although it is computationally expensive, it is a robust scheme.

5. TWO-DIMENSIONAL PROBLEM

The transport of a scalar quantity in a two-dimensional steady velocity field with speed $\mathbf{v} = (u, v)$ is given by

$$\frac{\partial c}{\partial t} + u\frac{\partial c}{\partial x} + v\frac{\partial c}{\partial y} = D_x\frac{\partial^2 c}{\partial x^2} + D_y\frac{\partial^2 c}{\partial y^2}, \quad 0 \le x \le L_x, \quad 0 \le y \le L_y, \quad t \in [0, T] \tag{16}$$

in which y is the second Cartesian co-ordinate direction and D_x, D_y are the constant diffusion coefficient is the x- and y-directions respectively. It has been demonstrated in the one-dimensional examples that it is when $Pe = \infty$, that numerical schemes will have difficulties. Therefore, in the two-dimensional example only $Pe = \infty$ will be considered. The analytical solution to this equation is simply the translation of the initial profile by the amount (uT, vT) without deformation.

Fractional stepping could be employed to solve the two-dimensional problem [53]. Equation (16) can be written in the form of Equation (2) in which the linear differential operator for the two dimensional problem is

$$\mathscr{C} = \mathscr{C}_{\mathrm{D}} + \mathscr{C}_{\mathrm{A}}$$

where $\mathscr{C}_{\mathrm{D}} = \mathscr{L}_{\mathrm{D}_x} + \mathscr{L}_{\mathrm{D}_y} = D_x(\partial^2/\partial x^2) + D_y(\partial^2/\partial y^2)$ and $\mathscr{C}_{\mathrm{A}} = \mathscr{L}_{\mathrm{A}_x} + \mathscr{L}_{\mathrm{A}_y} = -u(\partial/\partial x) - v(\partial/\partial y)$. Similar to the one-dimensional case, the exact solution is given by

$$c^{n+1} = \exp[\Delta t(\mathscr{C}_{\mathrm{D}} + \mathscr{C}_{\mathrm{A}})]c^n$$

The exponential term can be approximated to the desired order of accuracy. To first-order accuracy

$$c^{n+1} = \exp(\Delta t\mathscr{C}_{\mathrm{D}})\exp(\Delta t\mathscr{C}_{\mathrm{A}})c^n$$

Recalling that the quantities $\exp(\mathscr{L}_{\mathrm{A}_x})$ and $\exp(\mathscr{L}_{\mathrm{A}_y})$ are shift operators, then the analytical solution to the two dimensional problem is simply

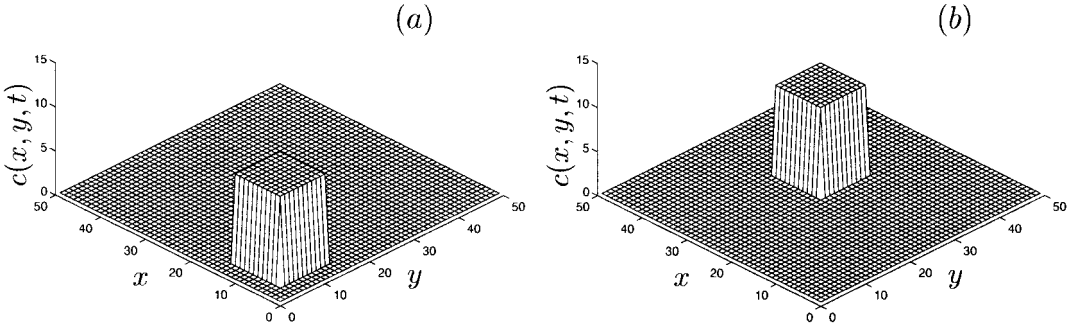

Figure 5. The initial (a) and exact (b) solution to the advection equation in two-dimensional flow.

$$c^{n+1} = \exp\left(D_x \Delta t \frac{\partial^2}{\partial x^2}\right) \exp\left(D_y \Delta t \frac{\partial^2}{\partial y^2}\right) c_\xi^n$$

where $\xi = x - u\Delta t,\ y - v\Delta t$. The first order quasi-characteristic formulation of the two-dimensional advective–diffusion equation is

$$c_{i,j}^{n+1} = c_{\xi_{i,j}}^n + D_x \Delta t \frac{\partial^2 c_{\xi_i}^n}{\partial x^2} + D_y \Delta t \frac{\partial^2 c_{\xi_i}^n}{\partial y^2} \tag{17}$$

Any bi-dimensional interpolation scheme could be used to solve Equation (17). Alternatively, the solution can be obtained by solving the one-dimensional equations

$$\bar{c}_{i,j}^{n+1} = c_{\xi_j}^n + D_y \Delta t \frac{\partial^2 c_{\xi_j}^n}{\partial y^2} \tag{18}$$

where $\xi_j = x_i,\ y_j - v\Delta t$ followed by

$$c_{i,j}^{n+1} = \bar{c}_{\xi_i}^{n+1} + D_x \Delta t \frac{\partial^2 \bar{c}_{\xi_i}^{n+1}}{\partial x^2} \tag{19}$$

where $\xi_i = x_i - u\Delta t,\ y_j$. The process consists of solving a one-dimensional problem in the x- and y-directions consecutively. Any suitable scheme can be used in the individual steps. As pointed out by the reviewer (Leonard) for uniform velocity fields in the x- and y-directions, the quasi-characteristic scheme using the integral of the concentration profile is conservative and constancy preserving. For more general solenoidal flow it is only conservative. Leonard *et al.* [54] suggest strategies so that a numerical scheme that uses operator splitting is both conservative and constancy preserving in solenoidal flow.

The two-dimensional problem consists of the pure advection of a rectangular parallelepiped. On the domain $[1, 50] \times [1, 50]$, with a uniform grid size $\Delta x = \Delta y = 1$ m, the parallelepiped is centered at (11, 11) with width $10\Delta x$ and $10\Delta y$. Its height is 10. The initial profile is shown in

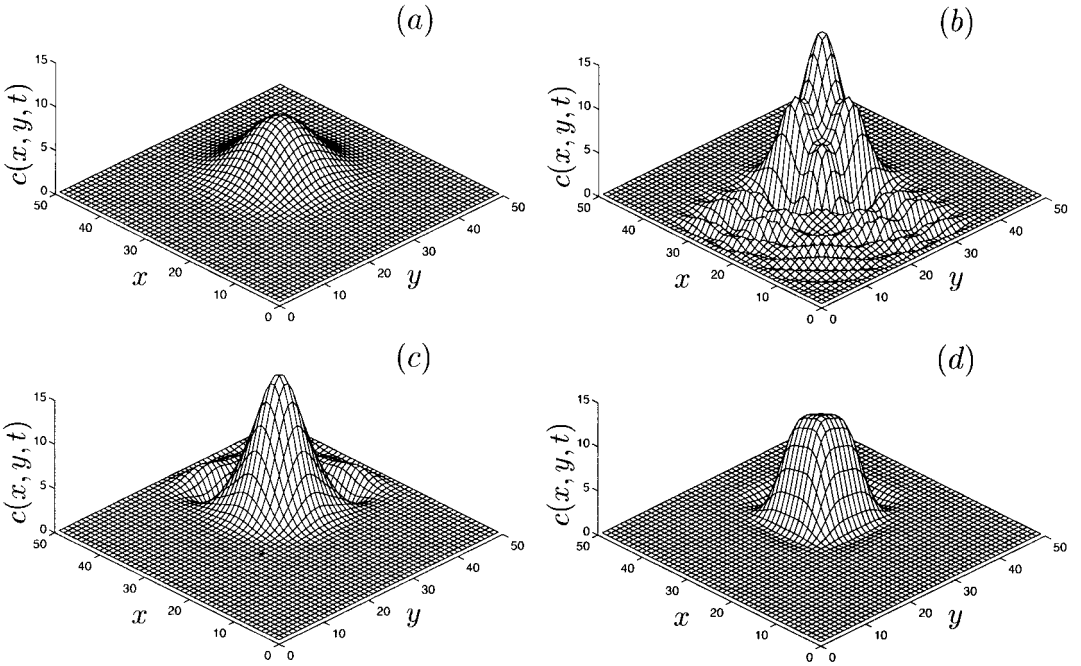

Figure 6. Advection in two-dimensional flow solved with $Cr = 0.1$ using naive finite differences schemes; (a) first-order upwinding, (b) Lax–Wendroff, (c) Warming–Beam, and (d) minimax scheme.

Figure 5(a). This profile is transported by the steady uniform velocity field $\mathbf{v} = (u, v)$, where $u = v = 0.1$ m s^{-1} to the location (30, 30) after $T = 200$ s. The exact solution to this problem is illustrated in Figure 5(b). In all the numerical schemes a computational time step $\Delta t = 1$ s was adopted. This provides a component Courant number of $Cr = 0.1$, which satisfies the stability constraints imposed on these schemes.

The two-dimensional test problem is solved using operator splitting with the first-order upwind scheme, which is shown in Figure 6(a); the second-order Lax–Wendroff, the Warming–Beam, and the minimax characteristics [55] schemes, which are shown in Figure 6(b)–(d) respectively; van Leer's second-order monotone upwind scheme [56], shown is Figure 7(a); Leonard's third-order upwind SHARP scheme [57], illustrated in Figure 7(b); and Roe's second-order monotone upwind scheme [58], where the flux is limited using Roe's superbee limiter, shown in Figure 7(c) The results of these schemes are compared with the results obtained from the quasi-characteristic scheme using an exponential spline interpolant fitted to the concentration, which are shown in Figure 7(d), and the exponential spline interpolant fitted to the integral of the concentration profile, shown in Figure 7(e).

The L_1-norm between the analytical and numerical solution of the test case has been calculated for all these schemes. These are given for the test problem in Table IV along with the maximum, the minimum computed concentration, and the computational time required by each scheme.

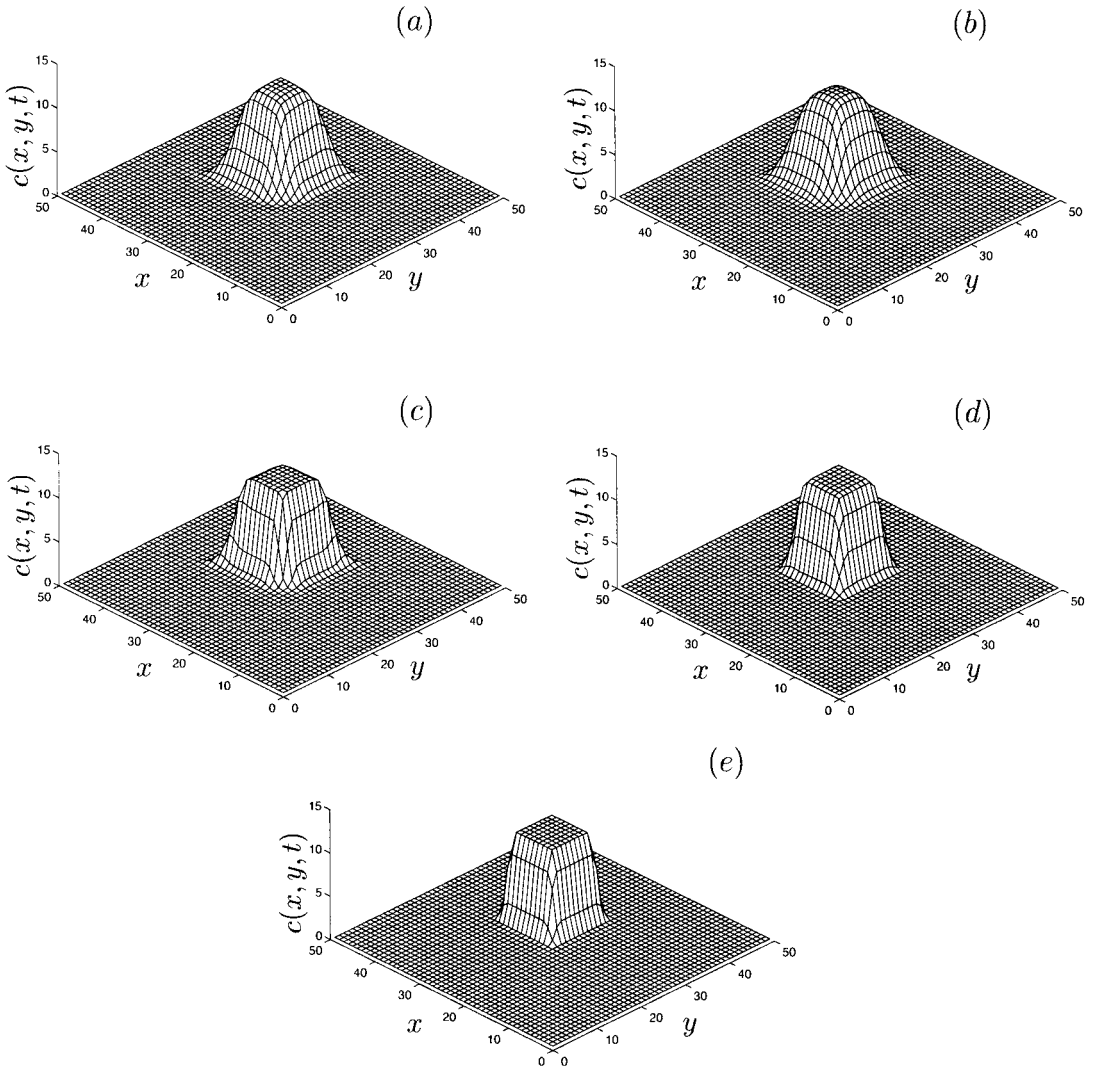

Figure 7. Advection in two-dimensional flow solved with $Cr = 0.1$ using slope or flux limiter schemes; (a) van Leer, (b) SHARP, (c) Roe, (d) quasi-characteristics with an exponential spline interpolant fitted to the concentration, and (e) quasi-characteristics with an exponential spline interpolant fitted to the integral of the concentration profile.

The highly diffusive first-order upwind scheme has produced a profile that is smeared and the peak concentration is attenuated. The solution does not contain oscillations, unlike the second-order Lax–Wendroff, the Warming–Beam, and the minimax schemes. Similar to the one-dimensional cases, the Lax–Wendroff scheme produces trailing waves and the

Table IV. Minimum, maximum, L_1-norm, and relative execution time for the solution of the two-dimensional advection equation of a rectangular profile using various schemes.

Numerical scheme	Minimum, $c_{\min}$	Maximum, $c_{\max}$	L_1	Relative CPU time
First-order upwindig	0.000	6.517	1.033294	1.000
Lax–Wendroff	−3.553	15.895	1.130739	1.388
Warming–Beam	−3.088	15.481	0.875083	1.333
Minimax	−0.845	11.613	0.459514	3.961
van Leer	0.000	9.930	0.441003	3.467
SHARP	−0.056	10.056	0.379688	5.855
Roe	0.000	10.000	0.229654	6.111
Characteristics with				
Exponential spline	0.000	10.000	0.256439	171/031
Integral	0.000	10.000	0.166308	104.389

Warming–Beam scheme introduces leading waves. The minimax scheme also produces strong leading waves and negative concentrations trailing the profile. All these second-order schemes overestimate the peak concentrations and produce negative concentrations. Overall, they are poor schemes for the solution of the advection equation.

The simulated profile is significantly improved with the use of flux limiters in a numerical scheme or by using higher-order schemes. The second-order upwind scheme of van Leer has not produced negative concentrations, is monotone, and has not introduced extraneous extrema but has introduced some smearing of the profile. The SHARP scheme although producing an improvement in the L_1-norm in comparison with the van Leer scheme, has produced negative concentrations and overestimates the maximum concentration. These results have been improved using Roe's upwind scheme. It has produced results that have preserved the properties of the exact solution. The maximum concentration has not been overestimated and the solution remains positive. It has captured the discontinuities in the profile with very little smearing of the profile.

The quasi-characteristic scheme using an exponential spline interpolant fitted to the concentration has also preserved the properties of the exact solution. Although it is not as accurate as the Roe upwinding scheme, because it introduces slightly more smearing of the discontinuities, it is one of the most accurate schemes used in this example. The most accurate scheme is the quasi-characteristics with an exponential spline interpolant fitted to the integral of the concentration profile. This scheme has produced the sharpest resolution of the discontinuity, which has been resolved over only four computational grid points.

Using exponential splin interoplation in a quasi-characteristic scheme results in a computationally expensive scheme, requiring at least and order of magnitude more computational effort than any other scheme. The computational effort reduces as *Pe* decrease and only slightly if the exponential spline interpolant is fitted to the integral of the concentration profile. The quasi-characteristic scheme, however, can be used to solve the advective–diffusion and advection equations. This is not the case for van Leer's scheme and Roe's scheme, which are restricted in this case to the advection equation.

6. CONCLUSIONS

Numerical schemes for the solution of the advective–diffusion which are based on the method of characteristics rely on some form of interpolation. These schemes are well known in meteorological modeling and in civil engineering applications. Unfortunately, many of these schemes employ interpolation schemes that do not preserve the properties of the solution or are highly diffusive. Like many finite difference schemes, they introduce oscillations in the solution near sharp changes in the profile.

A numerical scheme based on quasi-characteristics, which only requires spatial interpolation, is used to solve the advective–diffusion equation. In this scheme, shape preserving exponential spline interpolation is used. An iterative procedure is used to estimate the tension factors and to produce estimates of the nodal derivatives, which preserve certain properties of the data, required by the C^2 exponential spline interpolation. The exponential spline interpolant is accurate, robust and preserves the shape properties of the data. The accuracy of the quasi-characteristic method with shape preserving exponential spline interpolation has been demonstrated by solving the advective–diffusion equation in one and two dimensions. Although the construction of the shape-preserving interpolation scheme is computationally expensive, the numerical scheme is robust and produces sharp resolution of steep gradients and solutions free from extraneous oscillation. The computational effort required to solve the quasi-characteristic based scheme is at least an order of magnitude greater than other well-known schemes. This can be reduced by fitting the exponential spline interpolant to the integral of the concentration profile. The nodal concentrations are obtained by differentiating the interpolant. This produced a more accurate numerical scheme. The results indicate that there are advantages in using exponential spline interpolation in characteristic based numerical schemes.

REFERENCES

1. Chen Y, Falconer RA. Modified forms of the third-order convection, second-order diffusion scheme for the advection diffusion equation. *Advances in Water Resources* 1994; **17**: 147–170.
2. Falconer RA. Flow and water quality modelling in coastal and inland watee. *Journal of Hydraulic Research* 1991; **30**: 437–452.
3. Holly FM, Preissmann A. Accurate calculation of transport in two-dimensions. *Journal of Hydraulic Engineering ASCE* 1977; **103**: 1259–1277.
4. Li WH. *Differential Equations of Hydraulic Transients*, *Dispersion*, *and Ground Water Flow*. Prentice-Hall: Englewood Cliffs, NJ, 1972.
5. Hogarth WL, Noye BJ, Stagniti J, Parlange JY, Bolt G. A comparative study of finite difference methods for solving the one-dimensional transport equation with initial-boundary value discontinuity. *Computers and Mathematics with Applications* 1990; **20**: 67–82.
6. Comini G, Manzan M, Nonino C. Analysis of finite element schemes for convection-type problems. *International Journal for Numerical Methods in Fluids* 1995; **20**: 443–458.
7. Chen Y, Falconer RA. Advection–diffusion modelling using the modified QUICK scheme. *International Journal for Numerical Methods in Fluids* 1992; **15**: 1171–1196.
8. Tamamidis P, Assanis DN. Evaluation of various high-order-accuracy schemes with and without flux limiters. *International Journal of Numerical Methods in Fluids* 1993; **16**: 931–948.
9. Fenton JD. A family of schemes for computational hydraulics. *Proceedings of the 21st Congress of the International Association for Hydraulic Research*, Melbourne 1985; **2**: 23–27.
10. Bates JR, McDonald A. Multiply-upstream, semi-Lagrangian advective schemes: analysis and application to multi-level primitive equation model. *Monthly Weather Review* 1982; **110**: 1831–1842.

11. McDonald A. Accuracy of multiply-upstream, semi-Lagrangian advective. *Monthly Weather Review* 1984; **112**: 1267–1275.
12. Staniforth A, Côté J. Semi-Lagrangian schemes for atmospheric models—a review. *Monthly Weather Review* 1991; **119**: 2206–2223.
13. Bermejo R, Staniforth A. The conversion of semi-Lagrangian advection schemes to quasi-monotone schemes. *Monthly Weather Review* 1992; **120**: 2622–2632.
14. Holnicki P. A shape-preserving interpolation: applications to semi-Lagrangian advection. *Monthly Weather Review* 1995; **123**: 862–870.
15. Liu J, Pope A, Sepehrnoori K. A high-resolution finite-difference scheme for nonuniform grids. *Applied Mathematical Modelling* 1995; **19**: 162–172.
16. Leonard BP. Simple high-accuracy resolution program for convective modelling of discontinuities. *International Journal for Numerical Methods in Fluids* 1988; **8**: 1291–1318.
17. Holly FM, Komatsu T. Derivative approximations in the two-point fourth-order method for pollution transport. In *Proceedings of the Conference on Frontiers in Hydraulic Engineering*, Shen HT (ed.). American Society of Civil Engineers: New York, 1983; 349–355.
18. Prenter PM. *Splines and Variational Methods*. Wiley: New York, 1975.
19. McDonald A. Accuracy of multiply-upstream, semi-Lagrangian schemes'. *Monthly Weather Review* 1984; **112**: 1267–1275.
20. McCalpin JD. A quantitative analysis of the dissipation inherent in semi-Lagrangian advection. *Monthly Weather Review* 1988; **116**: 2330–2336.
21. Yang JC, Belleudy P, Temperville A. A higher-order Eulerian scheme for coupled advection-diffusion transport. *International Journal for Numerical Methods in Fluids* 1991; **12**: 43–58.
22. Holly FM, Usseglio-Polatera JM. Dispersion simulation in two-dimensional tidal flow. *Journal of Hydraulic Engineering ASCE* 1984; **110**: 905–926.
23. Yang JC, Hsu EL. On the use of the reach-back characteristics method for calculation of dispersion. *International Journal for Numerical Methods in Fluids* 1991; **12**: 225–235.
24. Chau KW, Lee JHW. A robust mathematical model for pollutant transportation in estuaries. *Journal of Water Resources* 1991; **168**: 63–80.
25. Holly FM, Toda K. Hybrid numerical scheme for linear and nonlinear advection. *Proceedings of the 21st Congress of the International Association for Hydraulic Research* 1985; **2**: 311–316.
26. Schohl GA, Holly FM. Cubic spline interpolation in Lagrangian advection computation. *Journal of Hydraulic Engineering ASCE* 1991; **117**: 248–253.
27. Renka RJ. Interpolatory tension splines with automatic selection of tension factors. *SIAM Journal for Scientific and Statistical Computing* 1987; **8**: 393–415.
28. Fritsch FN, Carlson RE. Monotone piecewise cubic interpolation. *SIAM Journal for Numerical Analysis* 1980; **17**: 238–246.
29. Fritsch FN, Butland J. A method for constructing local monotone piecewise cubic interpolants. *SIAM Journal for Scientific and Statistical Computing* 1984; **5**: 300–304.
30. de Boor C. *A Practical Guide to Splines*, *Applied Mathematical Sciences*, vol. 27. Springer: New York, 1978.
31. Cline AK. Scalar- and planar-valued curve fitting using splines under tension. *Association for Computing Machinery Communications* 1974; **17**: 218–220.
32. Rentrop P. An algorithm for the computation of the exponential spline. *Numerische Mathematik* 1980; **35**: 81–93.
33. Rentrop P, Wever U. Computation strategies for the tension parameters of the exponential splines. In *Conference on Optimal Control and Variational Calculus*, Bulirsch R, Miele A, Stoer J, Well K (eds). Springer: Berlin, 1986; 122–134.
34. Tornow V. An exponential spline interpolation for unequally spaced data points. *Computer Physics Communications* 1982; **28**: 61–67.
35. Wever U. Non-negative exponential splines. *Computer Aided Design* 1988; **20**: 11–16.
36. Akima H. A new method of interpolation and smooth curve fitting based on local procedures. *Journal of the Association of Computing Machinery* 1970; **17**: 589–602.
37. Hyman JM. Accurate monotonicity preserving cubic interpolation. *SIAM Journal for Scientific and Statistical Computing* 1983; **4**: 645–654.
38. Hyman JM. Accurate monotonicity preserving cubic interpolation. Los Alamos National Laboratory, Report LA-8796-MS, 1982.
39. Huynh HT. Accurate monotone cubic interpolation. *SIAM Journal for Numerical Analysis* 1993; **30**: 57–100.
40. Zoppu C. Numerical solution of the advective–diffusion equation. MSs thesis, Department of Mathematics, Australian National University, 1994.

41. Renka RJ. Algorithm 716: TSPACK: tension spline curve-fitting package. *Association of Computing Machinery Transactions on Mathematical Software* 1993; **19**: 81–94.
42. Abramowitz M, Stegun IA. *Handbook of Mathematical Functions with Formulas, Graphs, and Mathematical Tables*. Dover Publications: New York, 1972.
43. LeVeque RJ. *Numerical Methods for Conservation Laws*. Birkhauser: Basel, 1992.
44. Lax P, Wendroff B. Systems of conservation laws. *Communications on Pure and Applied Mathematics* 1960; **XIII**: 217–237.
45. Warming RF, Beam RM. Upwind second-order difference schemes and applications in aerodynamic flow. *American Institute of Aeronautics and Astronautics* 1976; **14**: 1241–1249.
46. Boris JP, Book DL. Flux-corrected transport. I. SHASTA, A fluid transport algorithm that works. *Journal of Computational Physics* 1973; **11**: 38–69.
47. Morrow R, Noye BJ. An implicit flux-corrected transport algorithm for both diffusion dominated and diffusion free conditions. In *Computational Techniques and Applications*, Noye BJ, Benjamin BR, Colgan LH (eds). Australian Mathematical Society: Canberra, 1992; 347–354.
48. Zalesak ST. Fully multidimensional flux-corrected transport algorithm for fluids. *Journal of Computational Physics* 1979; **31**: 335–362.
49. Leonard BP. The ULTIMATE conservative difference scheme applied to unsteady one-dimensional advection. *Computer Methods in Applied Mechanics and Engineering* 1991; **88**: 17–74.
50. Herriot JG, Reinsch CH. Algorithm 507: procedures for quintic natural spline interpolation. *Association of Computing Machinery Transactions on Mathematical Software* 1976; **2**: 281–289.
51. Warming RF, Hyett BJ. The modified equation approach to the stability and accuracy analysis of finite-difference methods. *Journal of Computational Physics* 1974; **14**: 159–179.
52. Leonard BP, Lock AP, MacVean MK. The NIRVANA scheme applied to one-dimensional advection. *International Journal for Numerical Methods in Heat and Fluid Flow* 1995; **5**: 341–377.
53. Strang G. On the construction and comparison of difference schemes. *SIAM Journal on Numerical Analysis* 1968; **5**: 506–517.
54. Leonard BP, Lock AP, MacVean MK. Conservative explicit unrestricted-time-step multidimensional constancy-preserving advection schemes. *Monthly Weather Review* 1996; **124**: 2588–2606.
55. Li CW. Advection–dispersion simulation by minimization characteristics and alternate direction–explicit methods. *Applied Mathematical Modeling* 1991; **15**: 616–623.
56. van Leer B. Towards the ultimate conservative difference scheme II: monotonicity and conservation combined in a second-order scheme. *Journal of Computational Physics* 1974; **14**: 361–370.
57. Leonard BP. Simple high-accuracy resolution program for convective modelling of discontinuities. *International Journal for Numerical Methods in Fluids* 1988; **8**: 1291–1318.
58. Roe PL. Approximate Riemann solvers, parameter vectors, and difference schemes. *Journal of Computational Physics* 1981; **43**: 357–372.

